

Gas Slippage in Partially Saturated Tight Rocks and During Drainage

Alexandra Amann-Hildenbrand^{1,*}, Mohammadebrahim Shabani¹, Thomas Hiller², Norbert Klitzsch³, Norbert Schleifer⁴, and Bernhard M. Krooss¹

¹ Institute of Geology and Geochemistry of Petroleum and Coal, Energy and Mineral Resources Group, RWTH-Aachen, Germany

² Leibniz Institute for Applied Geophysics, Hannover, Germany

³ Applied Geophysics and Geothermal Energy, E.ON Energy Research Center, RWTH-Aachen, Germany

⁴ Wintershall Holding GmbH, Barnstorf, Germany

Abstract. Effective gas permeability in partly water-saturated tight rocks is controlled by both, slippage and capillary effects. We present effective gas permeability coefficients measured on partially pre-saturated tight rock samples and during drainage starting from fully water-saturated samples. Measurements were made on Carboniferous (Westphalian D) and Permian (Rotliegend) tight sandstones with porosities <15% and permeability coefficients 10^{-16} m² (0.1 mDarcy). Plugs of 30 to 38 mm in diameter and up to 40 mm in length were used in this study in “triaxial” flow cells. Confining pressures ranged from 15 to 40 MPa and differential gas pressures up to 11 MPa were applied. Drainage of initially water-saturated samples was monitored by Nuclear Magnetic Resonance (NMR) in a flow-through cell. Additionally, gas flow experiments were run on samples with defined initial water saturations of up to 60%, established either by equilibration with water vapour or by centrifuging. Effective gas permeability coefficients increased by up to three orders of magnitude with decreasing water content. The experiments revealed that above a critical water saturation the effective permeability coefficients depend on drainage- and imbibition-controlled re-distribution of the water phase. Below this critical water saturation the apparent permeability coefficients of the gas are dominated by slippage effects.

1 Introduction

Gas slippage is a well-known phenomenon where the flow rate in narrow pores or capillaries exceeds that calculated with the assumption of viscous flow [1-2]. In this situation, the gas layer next to the pore surface is in motion with respect to the pore surface while Poiseuille’s law assumes zero velocity. The gas slippage effect increases as the mean free path length of the passing gas molecules approaches the scale of the transport pore size. It decreases with increasing gas pressure. In the “Klinkenberg diagram” the apparent gas permeability (k_{app}) is plotted as a function of the reciprocal mean pore pressure ($1/p_{mean}$). The Klinkenberg relationship

$$k_{app} = k_{inf} \cdot \left(1 + \frac{b}{p_{mean}}\right)$$

is used to determine the intrinsic or “liquid phase” permeability (k_{inf}) by linearly extrapolating the apparent permeability coefficients to the y-intercept at “infinitely” high gas pressures ($1/p_{mean} = 0$) [2]. The slip factor (b) is determined from the slope of the regression line.

Although the slippage effect has been well documented for single-phase gas flow, only few

experimental studies have investigated gas slippage in two-phase flow systems, especially for tight reservoirs [3-8]. Tight gas reservoirs contain water, either as connate/irreducible water or as imbibed water after drilling and hydraulic fracturing. Investigation of gas slippage in two-phase (gas-water) systems is therefore essential for the prediction of gas production rate from tight reservoirs [7].

In our experimental study, we have investigated the influence of water on gas flow mechanisms in tight gas reservoirs. Experiments were performed on partially pre-humidified sample plugs. Additionally, gas flow experiments (drainage and imbibition) were conducted, starting from fully water-saturated samples in an NMR flow cell. The dynamic water de- and re-saturation of the sample was continuously monitored by NMR measurements at each phase of the experiment.

* Corresponding author: alexandra.amann@emr.rwth-aachen.de

2 Sample preparation

2.1 Partial water saturation

The samples were pre-humidified in a desiccator at defined relative humidity (RH) levels by water vapour adsorption/desorption. Controlled RH in the desiccator was established by using saturated salt solutions of $MgCl_2$ (33%RH), $Mg(NO_3)_2$ (53%RH) and $NaCl$ (75%RH). Prior to moisture equilibration the samples were dried at 105 °C to constant weight. The water content was calculated from the weight increase after humidification. Assuming a water density of 1 g/cm³ the water saturation was then determined based on porosity values measured either by helium pycnometry or by saturation/buoyancy (Archimedes method).

2.2 Full water saturation

The sample plug after drying at 105 °C was placed overnight in a beaker inside an evacuated desiccator. The desiccator was then opened and degassed brine (here a 0.1 molar $MgSO_4$ solution) was admitted and allowed to invade the pore space at a slight overpressure (atmospheric pressure + 1 bar). The weight of the sample was monitored daily until it reached a constant value (full saturation). Due to the low permeability, the small pore diameters and the large sample size the saturation took several weeks.

3 Experimental procedure and results

3.1 Gas permeability measurements on partially saturated samples

Partially water-saturated samples were installed in a “triaxial” flow cell (Fig. 1). Axial and confining pressures were set to 20 MPa. Gas (helium) permeability measurements were performed on eight samples at a wide range of mean gas pressures (up to 12 MPa) for slip flow evaluation (Klinkenberg plot). The gas was passed through a high-pressure water reservoir (see Fig. 1) to avoid drying the samples and ensure that any changes in effective gas permeability were due only to water displacement (drainage) or slip flow. The measurements were performed using a steady state method; the upstream pressure was increased stepwise, while the downstream pressure remained atmospheric. Accordingly, also the pressure difference increased. After the gas permeability experiments the samples were weighed to determine any changes in water saturation.

The results of the apparent gas permeability measurements are shown for one selected sample at different degrees of water saturation (dry to 41%, Fig. 2). For all samples, the apparent gas permeability coefficients decreased by more than two orders of magnitude upon increase of water saturation to 30–45 % (Table 1). Normal Klinkenberg trends, i.e. positive linear relationships between apparent gas permeability and reciprocal mean gas pressure were found for samples in

the dry state and at low water-saturation (<25%). Here two different trends were observed: decrease or increase of the slippage factor b with increasing water saturation, (Fig. 3). In general, the slope always decreases with increasing water saturation.

For moist samples with higher water saturations (> 30%), the Klinkenberg plot of the apparent gas permeability coefficients showed negative trends. This phenomenon is caused by capillary drainage due to the successive increase in gas pressure difference in the course of the experiment.

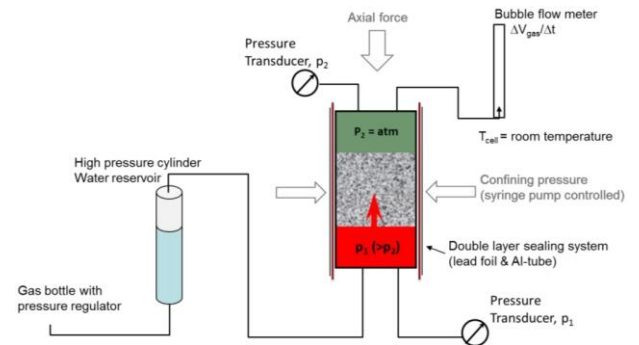


Fig. 1. Scheme of the experimental set-up used for permeability measurements on partially water-saturated samples

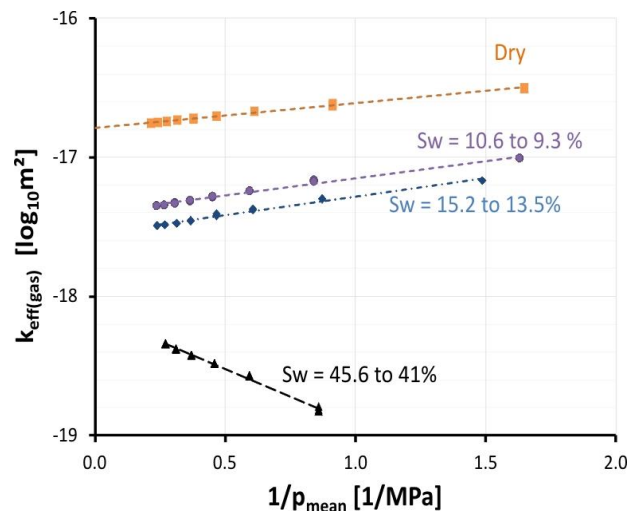


Fig. 2. Apparent effective gas (helium) permeability coefficients determined on the dry sample and at different water saturations.

Similar observations have been described in the literature. Rushing et al. [6] report a “decrease in gas slippage effects (as manifested by the decrease in line slope) with increasing water saturations”. However, as the “line slope” is the product of $k_{inf} \cdot b$ this assertion is misleading because their slippage-factors actually still increase with increasing water saturation. Similar results are given in Li et al., Reinecke and Sleep [5, 7, 8]. Estes et al. [10] observed decreasing slip factors for most of his samples. However, at higher water saturations also higher slippage-factors were determined, as well as negative slopes of the Klinkenberg regression line.

According to slip theory, the slip factor is inversely proportional to the pore diameter. Thus, an increase in slip factor indicates decreasing mean effective transport pore sizes. In the literature this is attributed to the presence of water films on the pore walls [11, 12] (“funicular flow”) [12]. In contrast, decreasing slip factors, thus increasing mean pore diameters, are considered to result from flow of gas in a completely separate network of gas-filled pores (“channel flow”) [12]. As the wetting phase will occupy the smallest capillaries, gas flow occurs in the open larger pore size fraction. Dullien [12] described these flow concepts based on direct microscopic observations in synthetic porous systems. In the present study, the presence of remaining water after drainage is considered to result in a shift of the NMR T2-signal towards nominally smaller pores (see chapter 3.2, Hiller et al., [13]). Both flow types may occur simultaneously, one being the dominating process, depending on pore size distribution and mineral composition, i.e. water suction pressure. This is an issue of ongoing research, and additional measurements are under way (N_2 adsorption, high pressure mercury injection and Cryo-BIB/SEM).

Table 1: Porosity and permeability coefficients of the samples analysed

Sample ID	Φ (%)	RH (%)	Sw_f (%)	k_{inf} (m^2)	b (MPa)
#1	9.7	0	0	2.2E-17	0.71
		33	9.1	3.7E-18	1.08
		55	13.7	2.4E-18	1.27
		75	44.1	5.9E-19	-1.03
#2	9.7	0	0	1.54E-17	0.62
		33	10.5	3.42E-18	1.16
		55	13.5	2.45E-18	1.19
		75	41.0	5.72E-19	-0.88
#3	10.6	0	0	4.90E-17	1.25
		33	5.2	7.74E-18	0.86
		55	8	6.41E-18	0.67
		75	27	1.23E-18	0.36
#4	6.1	0	0	3.60E-18	1.27
		33	3.7	2.12E-18	0.73
		55	1.2	2.57E-18	1.18
		75	2.5	2.21E-18	0.95
#5	3.4	0	0	6.84E-18	0.92
		55	3.2	5.01E-18	0.70
		55	3.2	6.31E-18	0.79
		75	3.0	3.17E-18	1.12
#6	5.1	0	0	3.3E-18	1.22
		55	3.8	2.4E-18	1.10
		55	5.7	2.0E-18	1.20
#7	10.7	0	0	4.22E-15	0.07
		55	2	4.2E-15	0.04
#8	1.3	0	0	2.03E-19	2.17
		55	62.9	1.06E-19	0.73
		55	43.4	1.20E-19	-0.97
#9	12.6	0	0	7.83E-18	0.5
		55	19	4.17E-18	0.3
		75	54	6.00E-20	-0.4

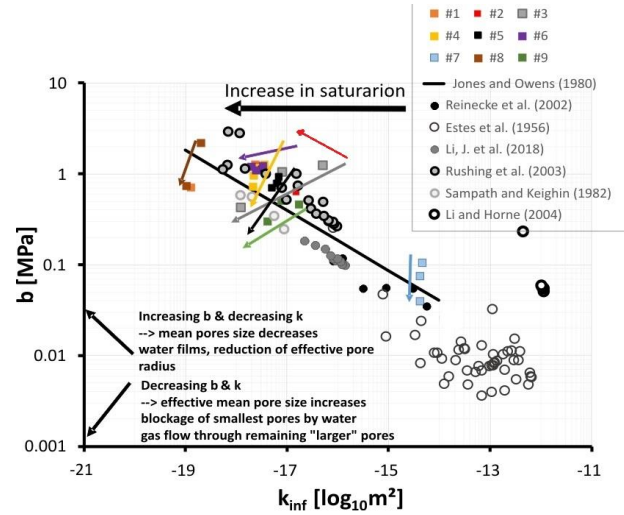


Fig. 3. Changes in slippage and permeability as a function of water saturation (Square symbols: data from this study for different samples, circles: Data from previous studies [4-6, 8, 10]. Arrows are inserted to guide the eye for the different trends.

3.2 Gas permeability measurements on initially fully water-saturated samples

Fully water-saturated samples were installed in an isostatic flow cell made out of NMR-inactive materials (Fig 4). The sample was placed between two Polyetheretherketone (PEEK) pistons surrounded by NMR-inactive confining fluid (Fluorinert FC-40). Flow-through measurements were performed at a confining pressure of 15 MPa. The flow experiments coupled with NMR measurement provide information on the dynamic water displacement in the sample plug.

The drainage experiment started by applying a constant pressure difference across the sample and monitoring NMR signal amplitudes and fluid flow. The NMR amplitudes at each stage were normalized to the NMR amplitude of the fully saturated sample to calculate water saturation. Gas permeability was determined either by a steady state (test # 1 and #2) or a non-steady state (test # 3) method. Details of the NMR flow cell setup and the technical protocol are given by Hiller et al. [13].

In the steady-state approach, the pressure difference (N_2 pressure up to 11MPa) across the sample was increased stepwise, resulting in successive desaturation (drainage experiment). This approach provides information on apparent gas permeability and water saturation as a function of the pressure difference. After each permeability test the sample plug was weighed and the change in water saturation compared with the water saturation measured by NMR.

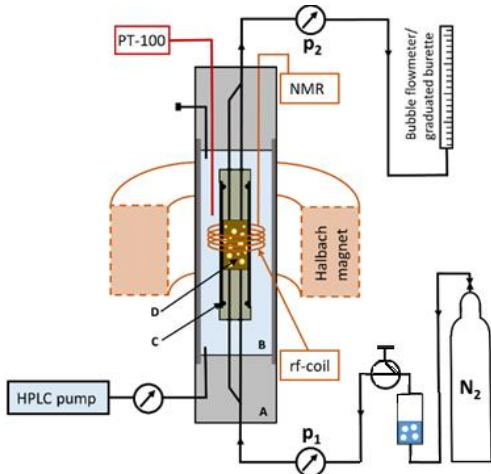


Fig. 4. Scheme of the NMR-inactive experimental set-up used for permeability measurements starting with fully water-saturated sample plugs. A – outer sealing system, B – confining pressure compartment filled with NMR-inactive oil, C – inner O-ring sealed sleeve system, D – sample placed between PEEK pistons.

In the non-steady state experiment, the gas pressure in the calibrated upstream volume was allowed to decrease, while downstream pressure remained atmospheric. The pressure on the upstream side was measured continuously and used to calculate the permeability coefficients. This method provides information on the spontaneous imbibition behaviour of the rock sample after gas breakthrough. Upon decrease in Δp and p_{mean} water imbibes back to the sample, resulting in an increase in saturation.

It should be noted that the pressure gradients during steady state and non-steady state experiments will result in saturation profiles along the sample, which, however, cannot be assessed/resolved with the procedures described here. The extent and consequences of these saturation profiles require further investigation.

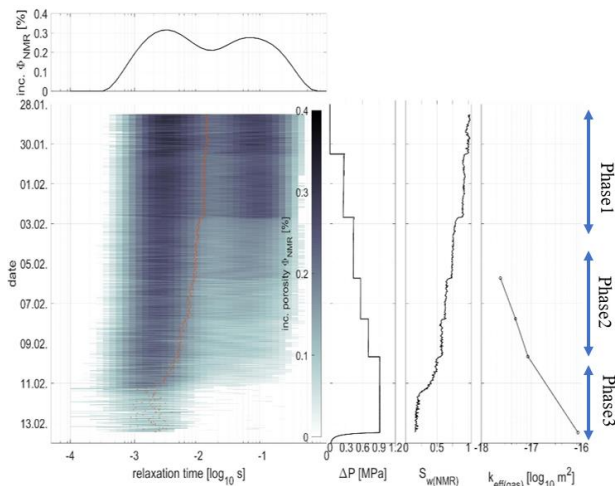


Fig. 5. NRM results obtained for test # 1. From left to right: Measured relaxation time distribution, Differential pressure

steps, saturation apparent effective gas permeability coefficients as a function of time.

Figs. 5 and 6 demonstrate the results of one steady state gas permeability experiment (test # 1). Water saturation decreased during the phase I of the experiments by drainage of the largest pores. However, no significant gas flow was observed at the downstream side during this phase. After gas breakthrough, the measured gas flow rate was used to calculate the apparent gas permeability (phase 2). These permeability values are nearly two orders of magnitude lower than those for the dry sample. Water saturation dropped significantly (to 25%) during phase 3 of the experiment leading to a one order of magnitude increase in apparent gas permeability reaching values close to the ones of the dry sample (Fig. 6). This indicates that at 25% water saturation the dominant conducting transport pathways were drained and that the remaining water-filled pores do not significantly contribute to the overall gas flow within the system.

As shown in Figure 6, apparent effective gas permeability coefficients increase with successive drainage, i.e. with increasing pressure difference, and with decreasing mean gas pressures. These observations are similar to those described in chapter 3.1 for samples with high water saturations. Two additional effects/trends were detected for other samples. For test # 2 (Figure 7) three different trends can be distinguished.

- (I) The capillary pressure-controlled flow regime, where mobile water is displaced and redistributed due to the increase in differential pressure.
- (II) The time delay effect, i.e. decreasing water saturation and increasing permeability until capillary pressure equilibrium has been reached.
- (III) The slip flow-dominated regime where effective apparent gas permeability coefficients decrease with increasing mean gas pressure. This regime prevails at lower water saturations, i.e. where the residual water is less mobile.

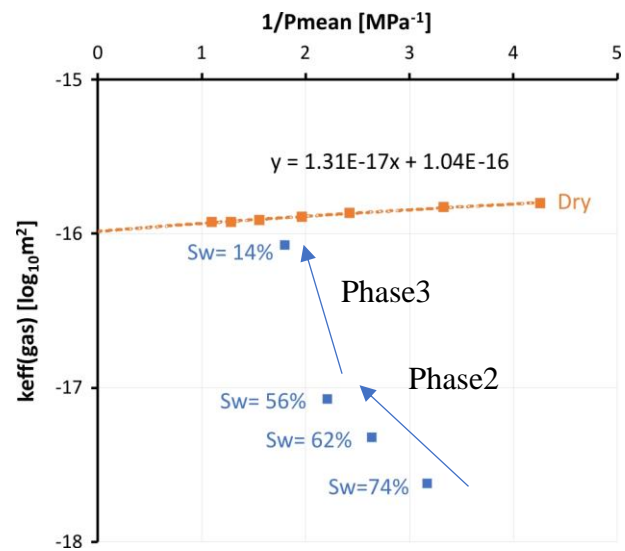


Fig. 6. Test # 1 - Klinkenberg plot showing apparent permeability coefficients measured on the dry sample and during the drainage experiment.

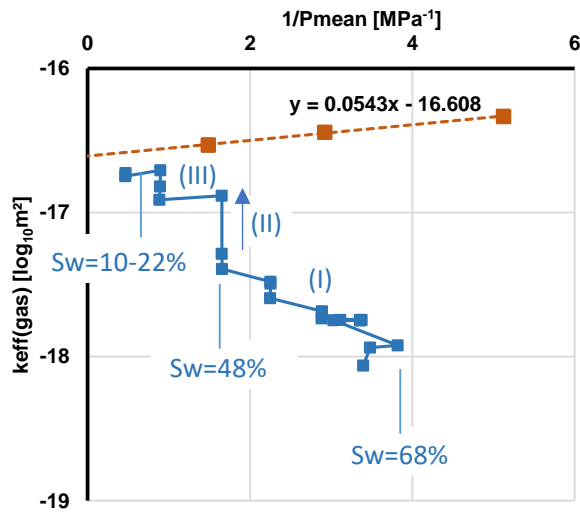


Fig. 7. Test #2 - Klinkenberg plot showing apparent permeability coefficients of the dry sample and effective apparent permeability coefficients during the drainage test. (I) capillary pressure-controlled drainage due to increase in differential pressure ($S_w=68-48\%$), (II) drainage – time delay, (III) slip flow-controlled gas flow at low water saturations ($S_w<48\%$)

Five drainage/imbibition cycles (non-steady state method) were performed on test #3 (Fig. 8). The experiment was initiated by applying a constant differential pressure across the sample. The first drainage/imbibition test started and changes in saturation during this cycle were monitored continuously. Due to technical problems, the gas flow was not monitored during this cycle. However, it was monitored during the other four drainage/imbibition cycles. After application of the initial pressure, gas flow starts and, as the top compartment is closed, the pressure difference across the sample decreases (Fig. 9a). As a result, water imbibes back into the pore system, resulting in an increase in water saturation and decrease of apparent gas permeability (up to two orders of magnitude, Fig. 8). The measured apparent gas permeability coefficients were up to three orders of magnitude lower than those measured on the dry sample (Fig. 9b).

As this system is controlled by capillary drainage, the negative Klinkenberg trends shown in Fig. 9b are clearly developed (cycle #4 and #5). For cycle #2 and #3 (higher water saturation), the trend is even more complex. Here, the negative slope is less pronounced at higher pressures (lower reciprocal mean pressure). Thereafter, permeability drops significantly, probably because imbibition is more efficient due to the higher amount of remaining water within the pore system. We are facing a very complex set of different processes acting simultaneously and partially with contrary effects: slip flow, drainage/imbibition, and likely some additional poro-mechanical response. Mechanical compressions at increasing effective stress, could result in a re-distribution of the pore water, i.e. driving water re-imbibition towards the compacted smaller pores.

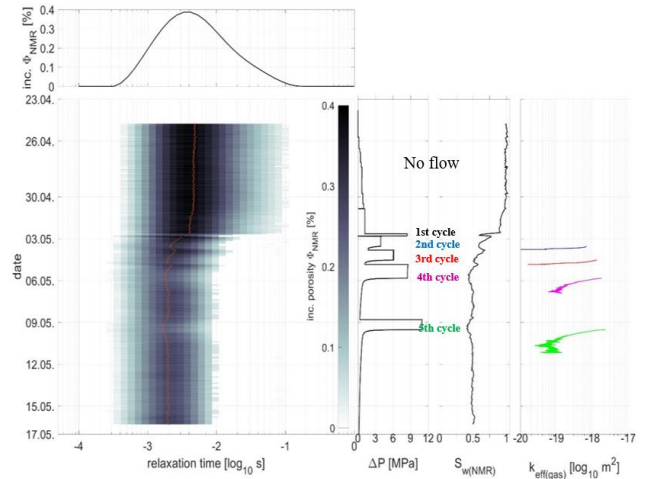


Fig. 8. Results from a non-steady state, imbibition test. The measured relaxation time distribution, upstream pressure, saturation, and apparent/effective gas permeability were recorded as a function of time.

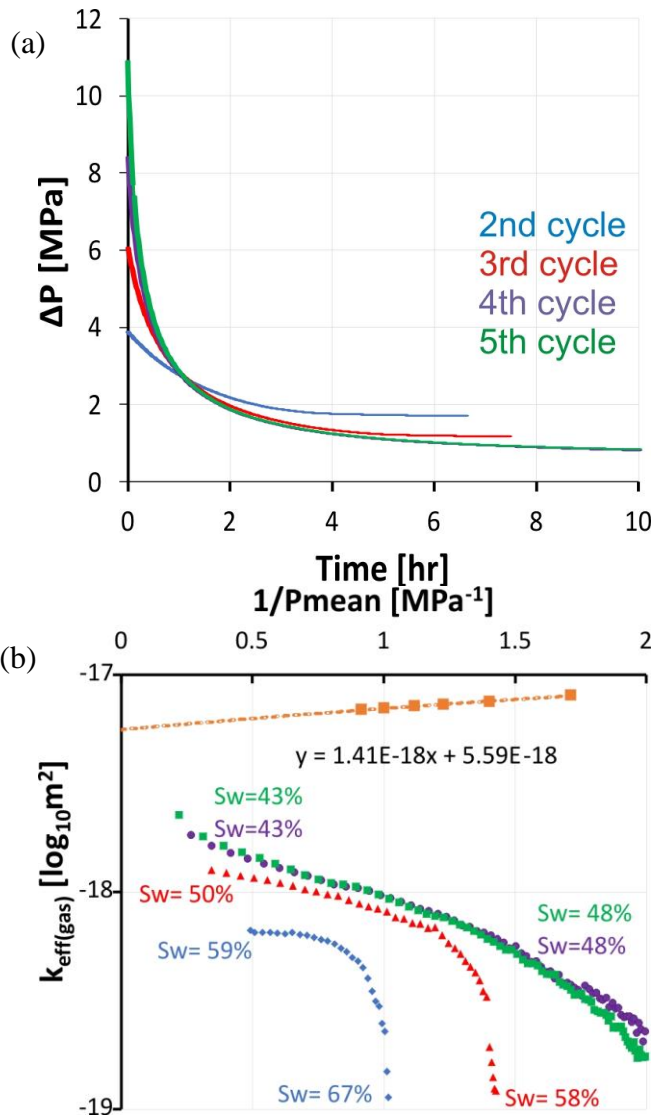


Fig. 8: Test #3 - Change of differential pressure for each drainage cycle as a function of time (a), Klinkenberg plot of

measured permeability coefficients in the dry and moist state (b).

4 Conclusions

In this study, apparent gas permeability measurements have been performed on partially and fully water-saturated samples. In both sets of experiments the effective gas permeability coefficients decreased by more than 3 orders of magnitude upon increasing water saturation.

At higher water saturations we observed that the apparent effective gas permeability coefficients follow a negative trend in the Klinkenberg plot. This is attributed to the capillary drainage effects, i.e. the displacement of the mobile water phase within increasing pressure difference.

At lower water saturations (below 30 %), we observed that the slope within the Klinkenberg plot is continuously decreasing with increasing water saturation. In contrast the slip factor either increases or decreases. This indicates that in the first case the effective average transport pore size is getting larger, in the latter case relatively lower. This is likely attributed to different water distribution within the pore system, however, this remains speculative with the current methods applied. Further research is ongoing, e.g. analyses by Cryo-BIB/SEM on partially water saturated samples.

5 Acknowledgements

The authors gratefully acknowledge Wintershall Holding GmbH for funding the iLoPS research project, within which this study was conducted. We also like to thank Jonas Kaiser and Gabriel Hoder for their valuable input and help with the experimental setup in the initial stage of the project.

References

1. A. Kundt, E. Warburg, "Über Reibung und Wärmeleitung verdünnter Gase," *Annalen der Physik* 231, 1875, 337-65.
2. L. Klinkenberg, "The permeability of porous media to liquids and gases," presented at *API In Drilling and production practice*, Tulsa, Okla., May 1941, pp. 200-213.
3. F.O. Jones, W.W. Owens, "A laboratory study of low-permeability gas sands," *Journal of Petroleum Technology* 32, 1980, 1631-140.
4. K. Sampath, C.W. Keighin, "Factors affecting gas slippage in tight sandstones of cretaceous age in the Uinta basin," *Journal of Petroleum Technology* 34, 1982, 2715-2720.
5. S.A. Reinecke, B.E. Sleep, "Knudsen diffusion, gas permeability, and water content in an unconsolidated porous medium," *Water Resources Research* 38, 2002, doi: 10.1029/2002WR001278.
6. J. Rushing, K. Newsham, K. Van Fraassen, "Measurement of the two-phase gas slippage phenomenon and its effect on gas relative permeability in tight gas sands," presented at *SPE Annual Technical Conference and Exhibition*, Denver, Colorado, USA, 5-8 Oct. 2003, SPE 84297.
7. K. Li, R.N. Horne, "Gas slippage in two-phase flow and the effect of temperature," presented at *SPE Western Regional Meeting*, Bakersfield, California, 26-30 March 2001, SPE 68778.
8. K. Li, R.N. Horne, "Experimental study of gas slippage in two-phase flow," presented at *SPE Western Regional Meeting*, Bakersfield, California, 26-30 March 2001, SPE 89038.
9. J. Li, Z. Chen, K. Wu, R. Li, J. Xu, Q. Liu, S. Qu, X. Li, "Effect of water saturation on gas slippage in tight rocks," *Fuel* 225, 2018, 519-32.
10. R.K. Estes, P.F. Fulton, "Gas Slippage and Permeability Measurements," *Journal of Petroleum Technology* 207, 1956, 69-73.
11. J. Li, Z. Chen, K. Wu, R. Li, J. Xu, Q. Liu, S. Qu, X. Li, "Effect of water saturation on gas slippage in tight rocks," *Fuel* 225, 2018, 519-532.
12. F.A.L. Dullien, "Porous Media: Fluid Transport and Pore Structure", 2nd edn, Academic Press, San Diego, 1992, 334-336
13. T. Hiller, G. Hoder, A. Amann-Hildenbrand, N. Klitzsch, N. Schleifer, "Two-Phase Fluid Flow Experiments Monitored by NMR," presented at *SCA2019*, Pau, France, 26-30 Aug. 2019, #117.